Pollutant emission reductions deliver decreased PM$_{2.5}$-caused mortality across China during 2015-2017

Ben Silver[1], Luke Conibear[1], Carly L. Reddington[1], Christoph Knote[2], Steve R. Arnold[1] and Dominick V. Spracklen[1]

5 [1] School of Earth and Environment, University of Leeds, Leeds, LS2 9JT, UK
[2] Meteorological Institute, Ludwig-Maximilians-University Munich, Theresienstr. 37, Munich, 80333, Germany

Correspondence to: Ben Silver (eebjs@leeds.ac.uk)

Abstract. Air pollution is a serious environmental issue and leading contributor to the disease burden in China. Rapid

10 reductions in fine particulate matter (PM$_{2.5}$) concentrations and increased ozone concentrations have occurred across China, during 2015 to 2017. We used measurements of particulate matter with a diameter < 2.5 µm (PM$_{2.5}$) and Ozone (O$_3$) from >1000 stations across China along with Weather Research and Forecasting model coupled with Chemistry (WRF-Chem) regional air quality simulations, to explore the drivers and impacts of observed trends. The measured nationwide median PM$_{2.5}$ trend of -3.4 µg m^{-3} year^{-1}, was well simulated by the model (-3.5 µg m^{-3} year^{-1}). With anthropogenic emissions fixed at 2015-

15 levels, the simulated trend was much weaker (-0.6 µg m^{-3} year^{-1}), demonstrating interannual variability in meteorology played a minor role in the observed PM$_{2.5}$ trend. The model simulated increased ozone concentrations in line with the measurements, but underestimated the magnitude of the observed absolute trend by a factor of 2. We combined simulated trends in PM$_{2.5}$ concentrations with an exposure-response function to estimate that reductions in PM$_{2.5}$ concentrations over this period have reduced PM$_{2.5}$-attribrutable premature morality across China by 150 000 deaths year^{-1}.

1 Introduction

20 Concentrations of particulate matter and ozone across China largely exceed international air quality standards (Reddington et al., 2019; Silver et al., 2018). This poor air quality is estimated to hasten the deaths of 870 000 - 2 470 000 people across China each year (Apte et al., 2015; Burnett et al., 2018; Cohen et al., 2017; Gu and Yim, 2016; Lelieveld et al., 2015). The Chinese government's efforts to improve air quality began in the 1990s, but emissions of pollutants continued to increase into the 21st century and air pollution worsened (Krotkov et al., 2016; Streets et al., 2008; Zhang et al., 2012). In 2013, China experienced

25 episodes of severe particulate matter pollution (Zhang et al., 2016). In response, the Chinese government announced the Action Plan on the Prevention and Control of Air Pollution which focused on the reduction of fine particulate matter (PM$_{2.5}$) through stringent emission controls during 2012-2017 (Zheng et al., 2017).

Atmospheric
Chemistry
and Physics
Discussions

1.1 Previous studies of trends in China's air quality

Satellite remote sensing studies have been used to show large changes in air pollution across China in recent decades, with
30 positive trends in Nitrogen Dioxide (NO_2) (Van der A et al., (2006), Sulphur Dioxide (SO_2) (Zhang et al., 2017) and $PM_{2.5}$
(Ma et al., 2016) during the 1990s and early 2000s. Trends in aerosol optical depth have been used to estimate changes in
$PM_{2.5}$, which peaked around 2011 (Ma et al., 2016). NO_2 across China peaked around 2011 (De Foy et al., 2016; Irie et al.,
2016), although concentrations in the Pearl River Delta (PRD) peaked earlier and western regions may have peaked later (Cui
et al., 2016). Several remote sensing studies show that SO_2 concentrations in China peaked around 2006 (Van Der A et al.,
35 2017; Krotkov et al., 2016; Zhang et al., 2017), matching the period of maximum emissions (Duan et al., 2016; Li et al., 2017;
Zheng et al., 2018). Analysis of measurements from the Acid Deposition Monitoring Network in East Asia (EANET) shows a
negative pH trend (i.e., becoming more acidic) from 1999 until a reversal occurs in 2006, matching peak SO_2 emissions and
concentrations (Duan et al., 2016). Measurements of O_3 concentrations at background monitoring sites indicate positive trends
in western China during 1994-2013 (Xu et al., 2016), and Taiwan during 1994-2003 (Chang and Lee, 2007), suggesting that
40 O_3 has been increasing across China during the past two decades. More recently, measurements at urban sites, also show
positive O_3 trends during 2005-2011 (Zhang et al., 2014).

The establishment of China's air pollution monitoring network, operated by the China National Environmental Monitoring
Centre (CNEMC) (Wang et al., 2015), which includes measurements from over 1600 locations, has enabled more detailed
analysis of recent air pollution changes (Silver et al., 2018; Zhai et al., 2019). Between 2015 and 2017, $PM_{2.5}$ concentrations
45 across China decreased by 28% (Silver et al., 2018). Zhai et al., (2019) reported a 30-40% decrease in $PM_{2.5}$ concentrations
during 2013-2017. In contrast O_3 concentrations have increased, with median concentration of O_3 across 74 key cities
increasing from 141 µg m3 in 2013 to 164 µg m3 in 2017 (Huang et al., 2018). Silver et al. (2018) found that O_3 maximum 8
h mean concentrations (O_3MDA8) increased by 4.6 % year-1 over 2015-2017. Positive regional O_3 trends remain even after
meteorological variability has been removed (Li et al., 2019a). Trends in NO_2 are more variable, with a negative trend reported
50 in eastern China and positive trends in western areas (Li and Bai, 2019). Silver et al., (2018) found that NO_2 had negative
trends in Hong Kong and North China Plain regions, but positive trends in the Yangtze River Delta (YRD), Sichuan Basin
(SCB) and PRD, and no overall trend at the national scale.

1.2 Identifying drivers of recent trends

Changes in the concentrations of air pollutants may be caused by changing emissions or by interannual variability of
55 meteorology. Stringent emission controls have started to reduce emissions of various pollutants across China. Between 2013
and 2017, emissions of $PM_{2.5}$, SO_2 and NO_x (NO_2 + Nitrogen Oxide) declined whereas emissions of Ammonia (NH_3) and Non-
Methane Volatile Organic Compounds (NMVOCs) remained fairly constant (Zheng et al., 2018). B. Zheng et al. (2018) also
demonstrate that emission reductions were primarily driven by pollution controls, rather than decreasing activity rates.
Meteorological variability alters atmospheric mixing, deposition and transport, all of which can influence the concentration of

60 pollutants. Separating the influence of meteorology and emissions on air pollutant concentrations is difficult, due to the interlinked nature of the chemistry-climate system (Jacob and Winner, 2009). However, to assess the efficacy of China's emissions reductions, it is necessary to separate these two factors.

There are two commonly used approaches to separate the influences of meteorology and emissions on variability in atmospheric pollutant abundances. The first approach uses statistical models, such as multi-linear regression, to control for the
65 influence of meteorology and allowing the proportion of air pollutant concentration variability that can be explained by meteorological variables to be calculated (Tai et al., 2010). The second approach is to use an atmospheric chemistry transport model to simulate pollutant concentrations. Through a comparison of multiple simulations, where either annual variability in emissions or meteorology are held constant, the relative influence of the two factors can be estimated. Here we analyse measurements and a regional air quality model to explore the role of changing anthropogenic emissions on air pollutant
70 concentrations and human health across China during 2015 to 2017.

2 Materials and Methods

2.1 Measurement dataset

We used hourly measurements from the CNEMC monitoring network (Wang et al., 2015) of $PM_{2.5}$, O_3, NO_2, and SO_2 for the period 2015-2017, which includes data from over 1600 monitoring stations across mainland China and is available to download
75 from http://beijingair.sinaapp.com/. This was combined with data from the Hong Kong Environmental Protection Department (https://cd.epic.epd.gov.hk/EPICDI/air/station/) and Taiwan's Environmental Protection Administration (https://taqm.epa.gov.tw/taqm/en/YearlyDataDownload.aspx). We conducted quality control on the measured data following the methods outlined in Silver et al. (2018). The cleaned dataset included measurements from 1155 sites.

2.2 WRF-Chem model setup

80 We used the Weather Research and Forecasting model with Chemistry (WRF-Chem) version 3.7.1 (Grell et al., 2005) to simulate trace gas and particulate pollution over China for 2015 to 2017. The model domain uses a Lambert Conformal grid (11-48 °N, 93-128 °E) centred on eastern China with a horizontal resolution of 30 km. The model has 33 vertical layers, with the lowest layer ~29 m above the surface, and the highest at 50 hPa (~19.6 km).

European Centre for Medium Range Weather Forecasts (ECMWF) ERA-Interim fields were used to provide meteorological
85 boundary and initial conditions, as well as to nudge the model temperature, winds and humidity above the boundary layer every 6 hours. Restricting nudging to above the boundary layer, allowed a more realistic representation of vertical mixing (Otte et al., 2012). Chemical boundary and initial conditions were provided by global fields from the Model for Ozone and Related Chemical Tracers version 4 (MOZART-4) chemical transport model (Emmons et al., 2010).

Anthropogenic emissions were from the Multi-resolution Emission Inventory for China (MEIC; www.meicmodel.org). MEIC
90 estimates emissions using a database of activity rates across residential, industrial, electricity generation, transportation and

agricultural emission sectors combined with China-specific emission factors (Hong et al., 2017). We used the 2015 MEIC dataset, then used sector-specific and species-specific scaling for 2016 and 2017 based on the emission totals estimated in B. Zheng et al. (2018). Table 1 shows emission totals for 2015, 2016 and 2017. Over the 2015 to 2017 period, Chinese emissions decreased by 38% for SO_2, 16% for $PM_{2.5}$ and 8% for NOx. For regions outside the MEIC dataset, we used anthropogenic

95   emissions from the EDGAR-HTAPv2.2 emission inventory for 2010.

Biogenic emissions were generated online by the Model of Emissions of Gases and Aerosol from Nature (MEGAN) (Guenther et al., 2000). Biomass burning emissions were provided by the Fire Inventory from NCAR (FINN) version 1.5 (Wiedinmyer et al., 2011), which uses satellite fire observations of fires and land cover to estimate daily 1 km^2 emissions. Dust emissions were generated online the Georgia Institute of Technology-Goddard Global Ozone Chemistry Aerosol Radiation and Transport

100   (GOCART) model with Air Force Weather Agency (AFWA) modifications (LeGrand et al., 2019).

Gas-phase chemistry is simulated using the MOZART-4 scheme and aerosol is treated by the Model for Simulating Aerosol Interactions and Chemistry (MOSAIC; Zaveri *et al.*, 2008) scheme, including grid-scale aqueous chemistry and an extended treatment of organic aerosol (Hodzic and Jimenez, 2011; Knote et al., 2014). Four discrete size bins were used within MOSAIC (0.039–0.156 μm, 0.156–0.625 μm, 0.625–2.5 μm, 2.5–10 μm) to represent the aerosol size distribution.

105   **2.3 Model and measurement trend estimation**

For comparison with the measurements, we sampled the model at the station locations using linear interpolation. Over 2015-2017, the model well simulated $PM_{2.5}$ (normalised mean bias (NMB) = 0.45), O_3 (NMB=-0.13) and SO_2 (NMB=0.07), while overestimating NO_2 concentrations by a factor of around 2 (NMB=1.17).

To separate the influence of changing anthropogenic emissions from interannual variability in meteorology, we conducted two

110   3-year simulations, both for 2015-2017. The first simulation (Control) included interannual variability in both anthropogenic emissions and meteorology. The second simulation (Fixed emissions) included interannual variability in meteorology, but with anthropogenic emissions fixed at 2015 levels.

Trends in the interpolated model data were calculated using the same method as the measurement data (Silver et al., 2018). The hourly data are averaged to monthly means, which are then deseasonalised. The magnitude and direction of linear trends

115   were calculated using the Theil-Sen estimator, a non-parametric method that is resistant to outliers (Carslaw, 2015). The Mann-Kendall test was used to assess the significance of trends, using a threshold of $p < 0.05$. This stage of the analysis was performed using the R package '*openair*' (Carslaw and Ropkins, 2012).

2.4 Health impact estimation

Health impacts are estimated for ambient $PM_{2.5}$ using the Global Exposure Mortality Model (GEMM) (Burnett et al., 2018).

120   We used the GEMM for non–accidental mortality (non–communicable disease, NCD, plus lower respiratory infections, LRI), using parameters including the China cohort (GBD 2017 Risk Factor Collaborators, 2018). For ambient O_3, we used the methodology of the Global Burden of Disease (GBD) study for 2017 (GBD 2017 Risk Factor Collaborators et al., 2018) to

estimate the mortality caused by chronic obstructive pulmonary disease. The United Nations adjusted population count dataset for 2015 at $0.05° \times 0.05□$ resolution was obtained from the Gridded Population of the World, Version 4 was used, along with

125 population age composition from GBD2017. Population count, population age, and baseline mortality rates were kept constant for 2015-2017 to estimate the variation due to changes in exposure only.

3 Measured and modelled trends comparison

3.1 Varying emissions scenario

Measured and simulated air quality trends over China during 2015 to 2017 largely compare well, and are shown in Figure 1

130 and 2. The measurements show widespread decline in $PM_{2.5}$ and SO_2 concentrations, widespread increase in O_3MDA8, and spatially variable trends in NO_2 concentrations, as reported previously (Silver et al., 2018). The model (Control simulation) simulates the widespread decline in $PM_{2.5}$ concentrations, with the median measured trend across China (-3.4 µg m^{-3} year^{-1}) well simulated by the model (-3.5 µg m^{-3} year^{-1}). In the measurements, 90% of significant trends are negative and 10% of significant trends are positive, with positive trends mostly being in the Fenwei Plain region, Jiangxi and Anhui. No significant

135 positive trends are simulated by the model, possibly due to coarse resolution of the model and the simplified scaling we apply to emissions for 2016 and 2017.

WRF-Chem captures the widespread increase in O_3MDA8, but underestimates the magnitude of the trend by a factor 2 (2.7 µg m^{-3} year^{-1} in the measurements, versus 1.3 µg m^{-3} year^{-1} simulated by WRF-Chem). WRF-Chem simulates negative O_3MDA8 trends in the Sichuan Basin and Taiwan, whereas in the measured data, all regions have positive median trends.

140 The measurements show zero overall median trend in NO_2 concentrations, with 46% of sites with significant trends being negative and 54% positive. In contrast, WRF-Chem simulates widespread reductions in NO_2 concentrations, with 100% of significant sites exhibiting negative trends and a negative nationwide median trend of -2.2 µg m^{-3} year^{-1}. The 7.0 % nationwide median decline in simulated NO_2 concentrations over 2015-2017, matches the 7.6 % decline in Chinese NOx emissions in the MEIC.

145 The measurements show a widespread decline in SO_2 concentrations, with a median nationwide trend of -1.9 µg m^{-3} year^{-1}. WRF-Chem captures the direction of the trend, but the magnitude of the trend is overestimated by a factor 2. The 32.5 % decline in simulated nationwide median SO_2 concentrations over 2015-2017, matches the 37.8 % decline in SO_2 emissions in the MEIC.

3.2 Fixed emissions scenario

150 The model simulation where anthropogenic emissions in China were fixed at 2015 levels has a weak negative $PM_{2.5}$ trend (-0.6 µg m^{-3} year^{-1}), a factor of six smaller than either the control simulation or the measurements (Figure 3). This suggests that the measured negative $PM_{2.5}$ trend has largely been driven by decreased anthropogenic emissions, with limited impact from

Atmospheric
Chemistry
and Physics
Discussions

interannual variability in meteorology. Chen et al. (2019) also concluded that emission reductions were the primary cause of reduced wintertime $PM_{2.5}$ across China during 2015-2017

155 The median O_3MDA8 trend in the fixed emission simulation is 0.0 µg m^{-3} year^{-1}. This suggests that interannual meteorological variation had no influence on O_3 trends at the China-wide scale during 2015-2017, which were largely driven by changing emissions. However, meteorological variability did drive regional changes in O_3. For example, in Guizhou, a trend of -2.5 µg m^{-3} year^{-1} was calculated in the fixed emissions simulation. Li et al. (2018) also report that the positive ozone trend over 2013 to 2017 is due to changes in anthropogenic emissions.

160 The fixed emission simulation also has a smaller NO_2 trend (-0.5 µg m^{-3}) compared to the control simulation (-2.2 µg m^{-3} year^{-1}), demonstrating emission reductions that are estimated in the MEIC are also the main reason for the negative simulated NO_2 trend. However, unlike $PM_{2.5}$ and O_3, the NO_2 trend calculated by the fixed emission simulation more closely matches measured trend. This may suggest that MEIC has overestimated the NO_2 emission reductions during 2015-2017. This suggestion is supported by recent satellite studies which found a slowing down or even reversal of NO_2 reductions during
165 2016-2019 (Li et al., 2019b), no significant trend in NO_2 during 2013-2017 (Huang et al., 2018), and increases in NO_2 concentration in the YRD, PRD and FWP regions during 2015-2017 (Feng et al., 2019). If NO_X emissions decline too strongly in MEIC, this may contribute to the simulated underestimate of the positive observed O_3MDA8 trend. Other work has suggested that increased O_3 concentrations are possibly linked to the rapid decline in aerosol (Li et al., 2019a).

4 Health impacts of changes to $PM_{2.5}$ and O_3 concentrations

170 ### 4.1 $PM_{2.5}$ health impacts

The control run simulated nation-wide population-weighted mean $PM_{2.5}$ concentration decreased by 12.8 % (10.1 µg m^{-3}), from 79.2 µg m^{-3} in 2015 to 69.1 µg m^{-3} in 2017. Greater decreases were simulated in more polluted and highly populated regions such as Beijing (-15.3 µg m^{-3}), Tianjin (-19.4 µg m^{-3}), Chongqing (province) (-14.2 µg m^{-3}) and Henan (-22.3 µg m^{-3}). Using the methodology of Burnett *et al.*, (2018), we estimate that mortality due to exposure to $PM_{2.5}$ decreased from 2 800
175 000 (CI: 2 299 000 – 3 302 000) premature mortalities in 2015, to 2 650 000 premature mortalities in 2017. The simulated reduction in $PM_{2.5}$ concentrations therefore reduced the number of premature mortalities attributable to $PM_{2.5}$ exposure by 150 000 (CI: 129 000 – 170 000) annual premature mortalities across China. The 12.8% reduction in $PM_{2.5}$ exposure only led to a 5% reduction in attributable mortality due to the non-linearity of the exposure-response function, which is less sensitive at higher exposure ranges (Conibear et al., 2018). The largest absolute reductions in premature mortality occur in Henan (15 000
180 deaths year^{-1}), Sichuan, Hebei and Tianjin (11 000 deaths year^{-1}) (Figure 4). The decline in $PM_{2.5}$ exposure also led to reduced morbidity with the Disability Adjusted Life Years (DALYs) rate per 100,000 population reduced from 159 to 150, with the largest changes occurring in central provinces such as (Supplementary Figure S3). Our results are comparable to Zheng *et al.*, (2017), who found that population weighted annual mean $PM_{2.5}$ concentrations decreased 21.5 % during 2013 – 2015, resulting in a premature mortality decrease of 120 000 deaths year^{-1}. Ding et al., (2019) estimated that during 2013-2017, a nationwide

185    $PM_{2.5}$ decrease of 9 µg m^{-3} caused premature mortalities pear year to decrease by 287 000, using the methodology from the GBD 2015 study, which estimates health impacts as having a weaker and less linear relationship to $PM_{2.5}$ concentrations.

4.2 O$_3$ health impacts

Increasing O$_3$ concentrations will result in an increase in health impacts that will act to offset some of the health benefits from declining $PM_{2.5}$ concentrations. WRF-Chem underestimated the observed magnitude of the O$_3$MDA8 trend during 2015-2017,

190   so the simulated change in health impacts would also be underestimated. However, our model bias in O$_3$ across China during 2015-2017 was reasonable (NMB=-0.13). To provide an estimate of the change in health impacts due to increasing O$_3$ concentrations we used simulated concentrations to estimate average health impacts due to exposure to O$_3$ over the 2015-2017 period, and then multiplied by the measured relative change in O$_3$MDA8. We estimate that exposure to O$_3$ caused an average of 143 000 (CI: 106 000 – 193 000) premature mortalities each year over 2015-2017. Assuming linear behaviour, the 15%

195   measured increase in O$_3$MDA8 would result in an increase of 21 000 premature mortalities per year. The exposure-outcome function is in reality sub-linear, so this is likely to be an overestimate. Regardless, this is substantially smaller than the 150 000 reduction in annual premature mortality due to reduced $PM_{2.5}$. We therefore suggest that changes in Chinese air pollution over 2015-2017 have likely had an overall beneficial impact on human health.

5 Conclusions

200   We used the WRF-Chem model to explore the drivers and impacts of changing air pollution across China during 2015-2017. A simulation with annually updated emissions was able to reproduce the measured negative trends in $PM_{2.5}$ concentrations over China during 2015 – 2017, while overestimating the negative trend in SO_2 and NO_2, and underestimating the positive trend in O$_3$. By comparing this with a simulation where emissions are held constant at 2015 levels, but meteorological forcing was updated, we show that interannual meteorological variation was not the main driver of the substantial trends in air

205   pollutants that were observed across China during 2015 – 2017. Our work shows that reduced anthropogenic emissions are the main cause of reduced $PM_{2.5}$ concentrations across China, suggesting that the Chinese government's 'Air Pollution Prevention and Control Action Plan' has been effective at starting to control particulate pollution. We estimate that the 12.8% reduction in population-weighted $PM_{2.5}$ concentrations that occurred during 2015-2017 has reduced premature mortality due to exposure to $PM_{2.5}$ by 5.3%, preventing 150 000 premature mortalities across China annually. Despite these substantial reductions, $PM_{2.5}$

210   concentrations still exceed air quality guidelines and cause negative impacts on human health. We estimate that exposure to O$_3$ during 2015-2017 causes on average 143 000 premature mortalities across China each year. Increases in O$_3$ concentration over 2015-2017, may have increased this annual mortality by about 20 000 premature mortalities per year, substantially less than the reduction in premature mortality due to declining particulate pollution. Changes in air pollution across China during 2015-2017 are therefore likely to have led to overall positive benefits to human health, amounting to a ~5 % reduction of the

215 ambient air pollution disease burden. However, to achieve larger reductions in the disease burden, further reductions in PM$_{2.5}$ concentrations are required, and pollution controls need to be designed that simultaneously reduce PM$_{2.5}$ and O$_3$ concentrations.

Data availability

Data used to create all figures are available in the supplement. Air quality measurement data from mainland China's monitoring network is available from http://beijingair.sinaapp.com/. Air quality measurement data from Hong Kong is available from

220 https://cd.epic.epd.gov.hk/EPICDI/air/station/. Air quality monitoring data from Taiwan is available from https://taqm.epa.gov.tw/taqm/en/YearlyDataDownload.aspx. Data from all WRF-Chem model simulations and post-processing codes are available from the corresponding author on request.

Author contributions

BS, CLR, DVS and SRA designed the research. BS performed the WRF-Chem model simulations, analysed all the model data

225 and wrote the manuscript. LC performed the health impact calculations. All authors contributed to scientific discussions and to the manuscript.

Competing interests

The authors declare that they have no conflict of interest.

Acknowledgements

References

van der A, R. J., Peters, D. H. M. U., Eskes, H., Boersma, K. F., Van Roozendael, M., De Smedt, I. and Kelder, H. M.: Detection of the trend and seasonal variation in tropospheric NO$_2$ over China, J. Geophys. Res. Atmos., doi:10.1029/2005JD006594, 2006.

240 Van Der A, R. J., Mijling, B., Ding, J., Elissavet Koukouli, M., Liu, F., Li, Q., Mao, H. and Theys, N.: Cleaning up the air: Effectiveness of air quality policy for SO2 and NO*x* emissions in China, Atmos. Chem. Phys., 17(3), 1775–1789, doi:10.5194/acp-17-1775-2017, 2017.

Apte, J. S., Marshall, J. D., Cohen, A. J. and Brauer, M.: Addressing Global Mortality from Ambient PM2.5, Environ. Sci. Technol., 49(13), 8057–8066, doi:10.1021/acs.est.5b01236, 2015.

245 Burnett, R., Chen, H., Szyszkowicz, M., Fann, N., Hubbell, B., Pope, C. A., Apte, J. S., Brauer, M., Cohen, A., Weichenthal, S., Coggins, J., Di, Q., Brunekreef, B., Frostad, J., Lim, S. S., Kan, H., Walker, K. D., Thurston, G. D., Hayes, R. B., Lim, C. C., Turner, M. C., Jerrett, M., Krewski, D., Gapstur, S. M., Diver, W. R., Ostro, B., Goldberg, D., Crouse, D. L., Martin, R. V, Peters, P., Pinault, L., Tjepkema, M., van Donkelaar, A., Villeneuve, P. J., Miller, A. B., Yin, P., Zhou, M., Wang, L., Janssen, N. A. H., Marra, M., Atkinson, R. W., Tsang, H., Quoc Thach, T., Cannon, J. B., Allen, R. T., Hart, J. E., Laden, F.,

250 Cesaroni, G., Forastiere, F., Weinmayr, G., Jaensch, A., Nagel, G., Concin, H., Spadaro, J. V and Spadaro, J. V.: Global estimates of mortality associated with long-term exposure to outdoor fine particulate matter., Proc. Natl. Acad. Sci. U. S. A., 115(38), 9592–9597, doi:10.1073/pnas.1803222115, 2018.

Carslaw, D.: The openair manual open-source tools for analysing air pollution data, King's Coll. London, (January), 287 [online] Available from: http://www.openair-project.org/PDF/OpenAir_Manual.pdf, 2015.

255 Carslaw, D. C. and Ropkins, K.: openair – Data Analysis Tools for the Air Quality Community, R J., 4(1), 20–29, 2012.

Chang, S. C. and Lee, C. Te: Evaluation of the trend of air quality in Taipei, Taiwan from 1994 to 2003, Environ. Monit. Assess., doi:10.1007/s10661-006-9262-1, 2007.

Chen, D., Liu, Z., Ban, J., Zhao, P. and Chen, M.: Retrospective analysis of 2015-2017 wintertime PM2.5 in China: Response to emission regulations and the role of meteorology, Atmos. Chem. Phys., doi:10.5194/acp-19-7409-2019, 2019.

260 Cohen, A. J., Brauer, M., Burnett, R., Anderson, H. R., Frostad, J., Estep, K., Balakrishnan, K., Brunekreef, B., Dandona, L., Dandona, R., Feigin, V., Freedman, G., Hubbell, B., Jobling, A., Kan, H., Knibbs, L., Liu, Y., Martin, R., Morawska, L., Pope, C. A., Shin, H., Straif, K., Shaddick, G., Thomas, M., van Dingenen, R., van Donkelaar, A., Vos, T., Murray, C. J. L. and Forouzanfar, M. H.: Estimates and 25-year trends of the global burden of disease attributable to ambient air pollution: an analysis of data from the Global Burden of Diseases Study 2015, Lancet, 389(10082), 1907–1918, doi:10.1016/S0140-

265 6736(17)30505-6, 2017.

Conibear, L., Butt, E. W., Knote, C., Arnold, S. R. and Spracklen, D. V.: Residential energy use emissions dominate health impacts from exposure to ambient particulate matter in India, Nat. Commun., doi:10.1038/s41467-018-02986-7, 2018.

Cui, Y., Lin, J., Song, C., Liu, M., Yan, Y., Xu, Y. and Huang, B.: Rapid growth in nitrogen dioxide pollution over Western China, Atmos. Chem. Phys, 16, 2005–2013, doi:10.5194/acp-16-6207-2016, 2016.

270 Ding, D., Xing, J., Wang, S., Liu, K. and Hao, J.: Estimated Contributions of Emissions Controls, Meteorological Factors, Population Growth, and Changes in Baseline Mortality to Reductions in Ambient PM2.5 and PM2.5-Related Mortality in China, 2013-2017, Environ. Health Perspect., doi:10.1289/EHP4157, 2019.

Duan, L., Yu, Q., Zhang, Q., Wang, Z., Pan, Y., Larssen, T., Tang, J. and Mulder, J.: Acid deposition in Asia: Emissions,

9

deposition, and ecosystem effects, Atmos. Environ., doi:10.1016/j.atmosenv.2016.07.018, 2016.

275   Emmons, L. K., Walters, S., Hess, P. G., Lamarque, J.-F., Pfister, G. G., Fillmore, D., Granier, C., Guenther, A., Kinnison, D., Laepple, T., Orlando, J., Tie, X., Tyndall, G., Wiedinmyer, C., Baughcum, S. L. and Kloster, S.: Geoscientific Model Development Description and evaluation of the Model for Ozone and Related chemical Tracers, version 4 (MOZART-4). [online] Available from: www.geosci-model-dev.net/3/43/2010/, 2010.

Feng, Y., Ning, M., Lei, Y., Sun, Y., Liu, W. and Wang, J.: Defending blue sky in China: Effectiveness of the "Air Pollution
280   Prevention and Control Action Plan" on air quality improvements from 2013 to 2017, J. Environ. Manage., 252, 109603, doi:10.1016/J.JENVMAN.2019.109603, 2019.

De Foy, B., Lu, Z. and Streets, D. G.: Satellite NO2 retrievals suggest China has exceeded its NOx reduction goals from the twelfth Five-Year Plan, Sci. Rep., 6, doi:10.1038/srep35912, 2016.

GBD 2017 Risk Factor Collaborators, Stanaway, J. D., Afshin, A., Gakidou, E., Lim, S. S., Abate, D., Abate, K. H., Abbafati,
285   C., Abbasi, N., Abbastabar, H., Abd-Allah, F., Abdela, J., Abdelalim, A., Abdollahpour, I., Abdulkader, R. S., Abebe, M., Abebe, Z., Abera, S. F., Abil, O. Z., Abraha, H. N., Abrham, A. R., Abu-Raddad, L. J., Abu-Rmeileh, N. M. E., Accrombessi, M. M. K., Acharya, D., Acharya, P., Adamu, A. A., Adane, A. A., Adebayo, O. M., Adedoyin, R. A., Adekanmbi, V., Ademi, Z., Adetokunboh, O. O., Adib, M. G., Admasie, A., Adsuar, J. C., Afanvi, K. A., Afarideh, M., Agarwal, G., Aggarwal, A., Aghayan, S. A., Agrawal, A., Agrawal, S., Ahmadi, A., Ahmadi, M., Ahmadieh, H., Ahmed, M. B., Aichour, A. N., Aichour,
290   I., Aichour, M. T. E., Akbari, M. E., Akinyemiju, T., Akseer, N., Al-Aly, Z., Al-Eyadhy, A., Al-Mekhlafi, H. M., Alahdab, F., Alam, K., Alam, S., Alam, T., Alashi, A., Alavian, S. M., Alene, K. A., Ali, K., Ali, S. M., Alijanzadeh, M., Alizadeh-Navaei, R., Aljunid, S. M., Alkerwi, A., Alla, F., Alsharif, U., Altirkawi, K., Alvis-Guzman, N., Amare, A. T., Ammar, W., Anber, N. H., Anderson, J. A., Andrei, C. L., Androudi, S., Animut, M. D., Anjomshoa, M., Ansha, M. G., Antó, J. M., Antonio, C. A. T., Anwari, P., Appiah, L. T., Appiah, S. C. Y., Arabloo, J., Aremu, O., Ärnlöv, J., Artaman, A., Aryal, K. K., Asayesh, H.,
295   Ataro, Z., Ausloos, M., Avokpaho, E. F. G. A., Awasthi, A., Quintanilla, B. P. A., Ayer, R., et al.: Global, regional, and national comparative risk assessment of 84 behavioural, environmental and occupational, and metabolic risks or clusters of risks for 195 countries and territories, 1990-2017: A systematic analysis for the Global Burden of Disease Stu, Lancet, doi:10.1016/S0140-6736(18)32225-6, 2018.

Grell, G. A., Peckham, S. E., Schmitz, R., McKeen, S. A., Frost, G., Skamarock, W. C. and Eder, B.: Fully coupled "online"
300   chemistry within the WRF model, Atmos. Environ., doi:10.1016/j.atmosenv.2005.04.027, 2005.

Gu, Y. and Yim, S. H. L.: The air quality and health impacts of domestic trans-boundary pollution in various regions of China, Environ. Int., 97, 117–124, doi:10.1016/j.envint.2016.08.004, 2016.

Guenther, A., Geron, C., Pierce, T., Lamb, B., Harley, P. and Fall, R.: Natural emissions of non-methane volatile organic compounds, carbon monoxide, and oxides of nitrogen from North America, Atmos. Environ., 34(12), 2205–2230,
305   doi:10.1016/S1352-2310(99)00465-3, 2000.

Hodzic, A. and Jimenez, J. L.: Geoscientific Model Development Modeling anthropogenically controlled secondary organic aerosols in a megacity: a simplified framework for global and climate models, Geosci. Model Dev, 4, 901–917,

doi:10.5194/gmd-4-901-2011, 2011.

Hong, C., Zhang, Q., He, K., Guan, D., Li, M., Liu, F. and Zheng, B.: Variations of China's emission estimates: Response to

310 uncertainties in energy statistics, Atmos. Chem. Phys., 17(2), 1227–1239, doi:10.5194/acp-17-1227-2017, 2017.

Huang, J., Pan, X., Guo, X. and Li, G.: Health impact of China's Air Pollution Prevention and Control Action Plan: an analysis of national air quality monitoring and mortality data, Lancet Planet. Heal., doi:10.1016/S2542-5196(18)30141-4, 2018.

Irie, H., Muto, T., Itahashi, S., Kurokawa, J. and Uno, I.: Turnaround of Tropospheric Nitrogen Dioxide Pollution Trends in China, Japan, and South Korea, Sola, 12(0), 170–174, doi:10.2151/sola.2016-035, 2016.

315 Jacob, D. J. and Winner, D. A.: Effect of climate change on air quality, Atmos. Environ., 43(1), 51–63, doi:10.1016/j.atmosenv.2008.09.051, 2009.

Knote, C., Hodzic, A., Jimenez, J. L., Volkamer, R., Orlando, J. J., Baidar, S., Brioude, J., Fast, J., Gentner, D. R., Goldstein, A. H., Hayes, P. L., Knighton, W. B., Oetjen, H., Setyan, A., Stark, H., Thalman, R., Tyndall, G., Washenfelder, R., Waxman, E. and Zhang, Q.: Simulation of semi-explicit mechanisms of SOA formation from glyoxal in aerosol in a 3-D model, Atmos.

320 Chem. Phys., 14(12), 6213–6239, doi:10.5194/acp-14-6213-2014, 2014.

Krotkov, N. A., McLinden, C. A., Li, C., Lamsal, L. N., Celarier, E. A., Marchenko, S. V., Swartz, W. H., Bucsela, E. J., Joiner, J., Duncan, B. N., Folkert Boersma, K., Pepijn Veefkind, J., Levelt, P. F., Fioletov, V. E., Dickerson, R. R., He, H., Lu, Z. and Streets, D. G.: Aura OMI observations of regional SO2 and NO2 pollution changes from 2005 to 2015, Atmos. Chem. Phys., 16(7), 4605–4629, doi:10.5194/acp-16-4605-2016, 2016.

325 LeGrand, S. L., Polashenski, C., Letcher, T. W., Creighton, G. A., Peckham, S. E. and Cetola, J. D.: The AFWA dust emission scheme for the GOCART aerosol model in WRF-Chem v3.8.1, Geosci. Model Dev., doi:10.5194/gmd-12-131-2019, 2019.

Lelieveld, J., Evans, J. S., Fnais, M., Giannadaki, D. and Pozzer, A.: The contribution of outdoor air pollution sources to premature mortality on a global scale, Nature, 525(7569), 367–371, doi:10.1038/nature15371, 2015.

Li, K. and Bai, K.: Spatiotemporal Associations between PM2.5 and SO2 as well as NO2 in China from 2015 to 2018, Int. J.

330 Environ. Res. Public Health, 16(13), 2352, doi:10.3390/ijerph16132352, 2019.

Li, K., Jacob, D. J., Liao, H., Shen, L., Zhang, Q. and Bates, K. H.: Anthropogenic drivers of 2013–2017 trends in summer surface ozone in China, Proc. Natl. Acad. Sci. U. S. A., doi:10.1073/pnas.1812168116, 2019a.

Li, M., Liu, H., Geng, G., Hong, C., Liu, F., Song, Y., Tong, D., Zheng, B., Cui, H., Man, H., Zhang, Q. and He, K.: Anthropogenic emission inventories in China: A review, Natl. Sci. Rev., doi:10.1093/nsr/nwx150, 2017.

335 Li, R., Bo, H. and Wang, Y.: Slowing-down reduction and Possible Reversal Trend of Tropospheric NO2 over China during 2016 to 2019, [online] Available from: http://arxiv.org/abs/1907.06525 (Accessed 23 September 2019b), 2019.

Ma, Z., Hu, X., Sayer, A. M., Levy, R., Zhang, Q., Xue, Y., Tong, S., Bi, J., Huang, L. and Liu, Y.: Satellite-based spatiotemporal trends in PM2.5concentrations: China, 2004-2013, Environ. Health Perspect., 124(2), 184–192, doi:10.1289/ehp.1409481, 2016.

340 Otte, T. L., Nolte, C. G., Otte, M. J. and Bowden, J. H.: Does nudging squelch the extremes in regional climate modeling?, J. Clim., doi:10.1175/JCLI-D-12-00048.1, 2012.

Reddington, C. L., Conibear, L., Knote, C., Silver, B. J., Arnold, S. R. and Spracklen, D. V.: Exploring the impacts of anthropogenic emission sectors on PM<sub>2.5</sub> and human health in South and East Asia, Atmos. Chem. Phys. Discuss., doi:10.5194/acp-2019-147, 2019.

345 Silver, B., Reddington, C. L., Arnold, S. R. and Spracklen, D. V.: Substantial changes in air pollution across China during 2015-2017, Environ. Res. Lett., doi:10.1088/1748-9326/aae718, 2018.

Streets, D. G., Yu, C., Wu, Y., Chin, M., Zhao, Z., Hayasaka, T. and Shi, G.: Aerosol trends over China, 1980–2000, Atmos. Res., 88(2), 174–182, doi:10.1016/J.ATMOSRES.2007.10.016, 2008.

Tai, A. P. K., Mickley, L. J. and Jacob, D. J.: Correlations between fine particulate matter (PM2.5) and meteorological variables
350 in the United States: Implications for the sensitivity of PM2.5 to climate change, Atmos. Environ., 44(32), 3976–3984, doi:10.1016/j.atmosenv.2010.06.060, 2010.

Wang, S., Li, G., Gong, Z., Du, L., Zhou, Q., Meng, X., Xie, S. and Zhou, L.: Spatial distribution, seasonal variation and regionalization of PM2.5 concentrations in China, Sci. China Chem., doi:10.1007/s11426-015-5468-9, 2015.

Wiedinmyer, C., Akagi, S. K., Yokelson, R. J., Emmons, L. K., Al-Saadi, J. A., Orlando, J. J. and Soja, A. J.: The Fire
355 INventory from NCAR (FINN): A high resolution global model to estimate the emissions from open burning, Geosci. Model Dev., 4(3), 625–641, doi:10.5194/gmd-4-625-2011, 2011.

Xu, W., Lin, W., Xu, X., Tang, J., Huang, J., Wu, H. and Zhang, X.: Long-term trends of surface ozone and its influencing factors at the Mt Waliguan GAW station, China-Part 1: Overall trends and characteristics, Atmos. Chem. Phys., 16(10), 6191–6205, doi:10.5194/acp-16-6191-2016, 2016.

360 Zaveri, R. A., Easter, R. C., Fast, J. D. and Peters, L. K.: Model for Simulating Aerosol Interactions and Chemistry (MOSAIC), J. Geophys. Res. Atmos., doi:10.1029/2007JD008782, 2008.

Zhai, S., Jacob, D. J., Wang, X., Shen, L., Li, K., Zhang, Y., Gui, K., Zhao, T. and Liao, H.: Fine particulate matter (PM<sub>2.5</sub>) trends in China, 2013–2018: separating contributions from anthropogenic emissions and meteorology, Atmos. Chem. Phys., doi:10.5194/acp-19-11031-2019, 2019.

365 Zhang, H., Wang, S., Hao, J., Wang, X., Wang, S., Chai, F. and Li, M.: Air pollution and control action in Beijing, J. Clean. Prod., 112, 1519–1527, doi:10.1016/j.jclepro.2015.04.092, 2016.

Zhang, L., Lee, C. S., Zhang, R. and Chen, L.: Spatial and temporal evaluation of long term trend (2005–2014) of OMI retrieved NO2and SO2concentrations in Henan Province, China, Atmos. Environ., doi:10.1016/j.atmosenv.2016.11.067, 2017.

Zhang, Q., Geng, G. N., Wang, S. W., Richter, A. and He, K. Bin: Satellite remote sensing of changes in NO x emissions over
370 China during 1996-2010, Chinese Sci. Bull., 57(22), 2857–2864, doi:10.1007/s11434-012-5015-4, 2012.

Zhang, Q., Yuan, B., Shao, M., Wang, X., Lu, S., Lu, K., Wang, M., Chen, L., Chang, C. C. and Liu, S. C.: Variations of ground-level O3 and its precursors in Beijing in summertime between 2005 and 2011, Atmos. Chem. Phys., doi:10.5194/acp-14-6089-2014, 2014.

Zheng, B., Tong, D., Li, M., Liu, F., Hong, C., Geng, G., Li, H., Li, X., Peng, L., Qi, J., Yan, L., Zhang, Y., Zhao, H., Zheng,
375 Y., He, K. and Zhang, Q.: Trends in China's anthropogenic emissions since 2010 as the consequence of clean air actions,

Atmos. Chem. Phys. Discuss., (X), 1–27, doi:10.5194/acp-2018-374, 2018.

Zheng, Y., Xue, T., Zhang, Q., Geng, G., Tong, D., Li, X. and He, K.: Air quality improvements and health benefits from China's clean air action since 2013, Environ. Res. Lett., 12(11), doi:10.1088/1748-9326/aa8a32, 2017.

380   **Table 1. Chinese pollutant emissions (Tg yr^{-1}) during 2015 to 2017 from MEIC.**

|	SO_2	NO_x	NMVOC	NH_3	CO	TSP	PM_{10}	$PM_{2.5}$	BC	OC	CO_2
2015	16.9	23.7	28.6	10.5	153.6	21.9	12.3	9.1	1.4	2.5	10347.2
2016	13.4	22.5	28.4	10.2	142	17.9	10.8	8.1	1.3	2.3	10290.7
2017	10.5	21.9	28.6	10.2	136.2	16.7	10.2	7.6	1.2	2.1	10434.3

385

390
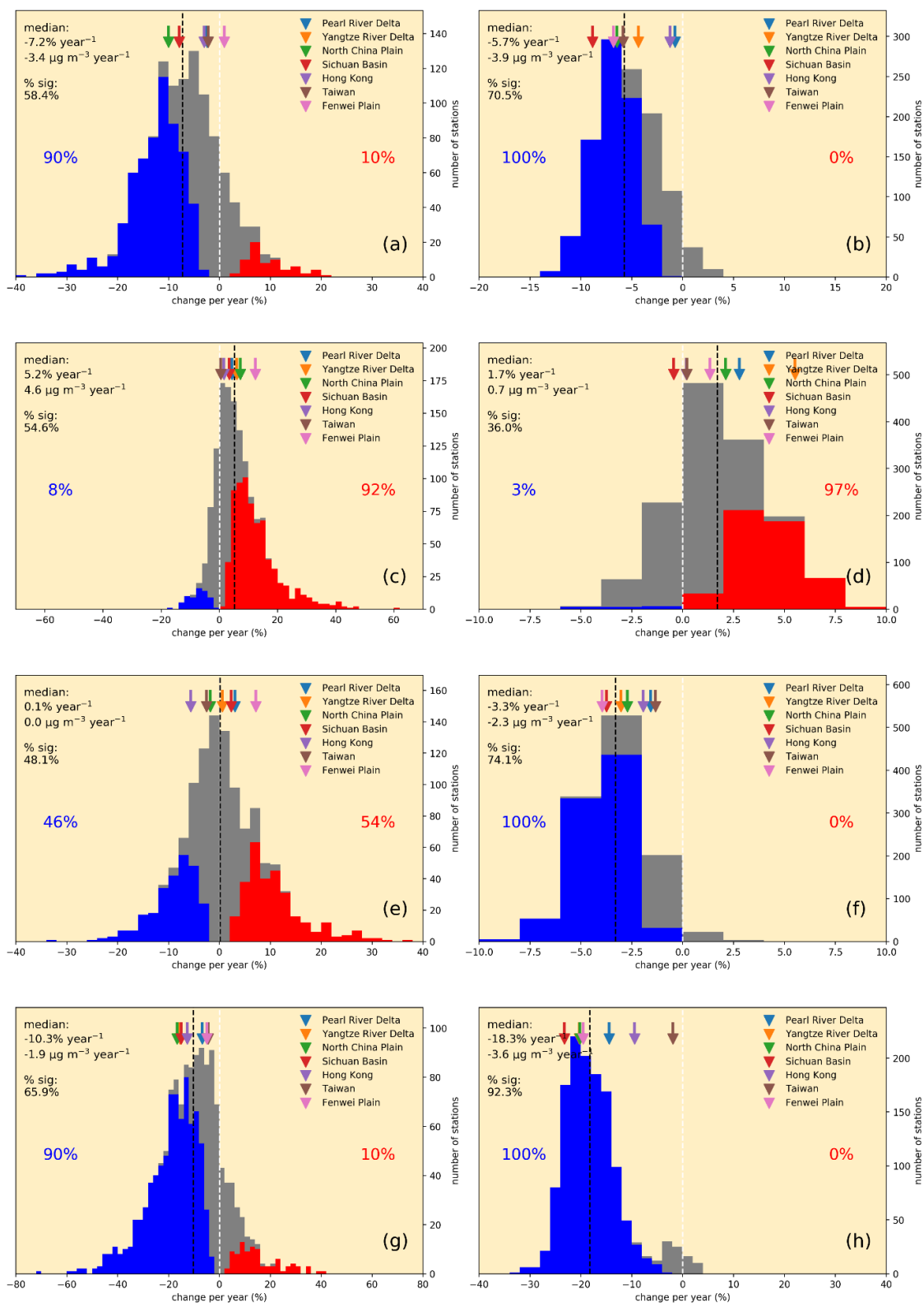
Figure 1: Histograms showing the frequency distribution of trends in concentrations of (a,b) PM$_{2.5}$, (c,d) O$_3$MDA8, (e,f) NO$_2$, (g,h) SO$_2$ across China and Taiwan during 2015–2017. Measured trends (left hand panels) are compared to simulated trends (right hand panels). The median relative and absolute trend as well as the percentage of stations with significant trends is shown on each panel. The percentage of significant trends that are negative (blue) or positive (red) are also shown. The black dotted line shows the median trend across all sites, while the white dotted line shows zero. Arrows show the median trend for the regional domain: Pearl River Delta (PRD), Yangtze River Delta (YRD), North China Plain (NCP), Sichuan Basin (SCB), Hong Kong (HK), Taiwan (TW) and the Fenwei Plain (FWP).
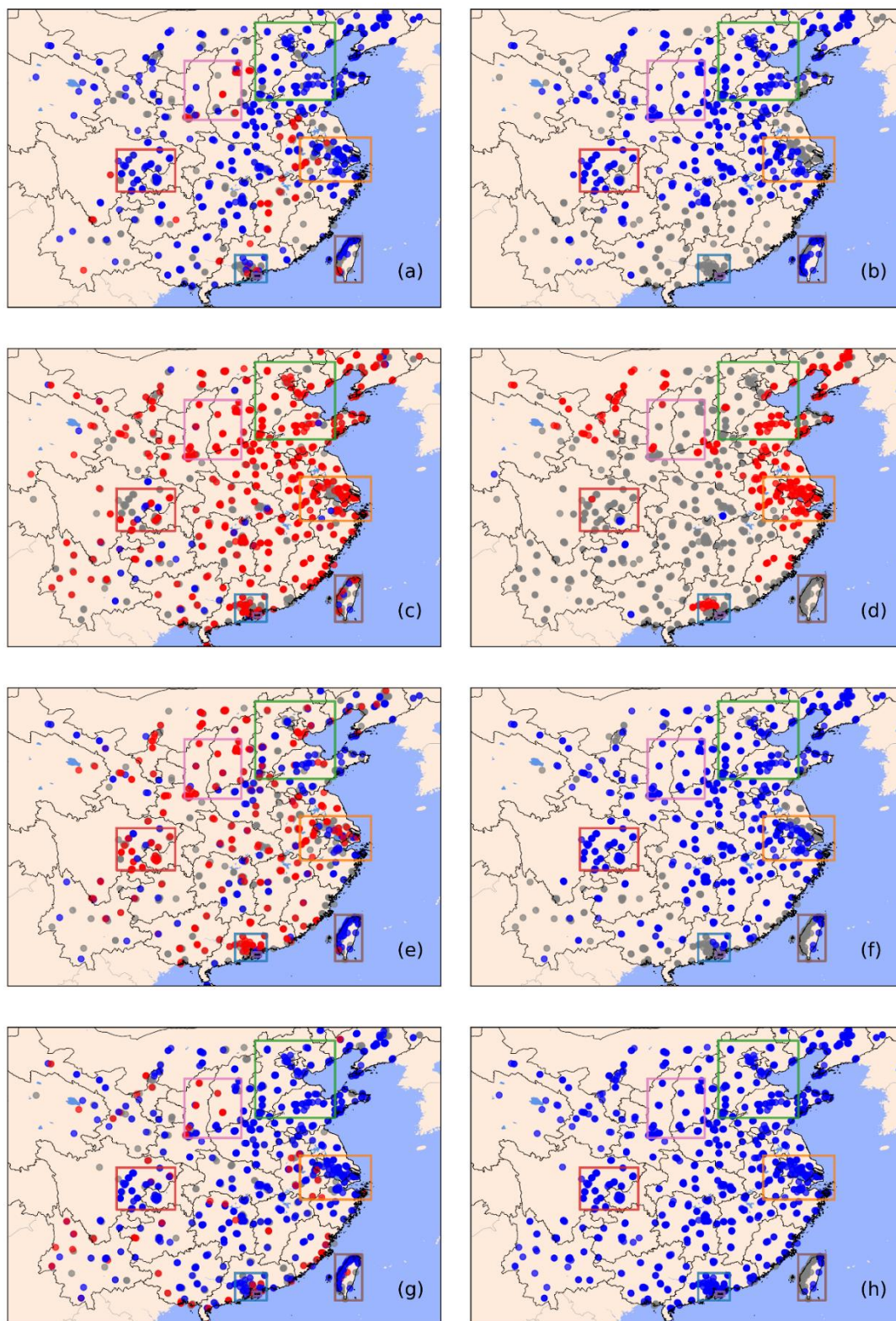
**Figure 2. Map showing the spatial distribution of trends in concentrations of (a,b) PM$_{2.5}$, (c,d) O$_3$MDA8, (e,f) NO$_2$, (g,h) SO$_2$ across China and Taiwan during 2015–2017. Measured trends (left hand panels) are compared to simulated trends (right hand panels). Red indicates a significant positive trend, whereas blue indicates a significant negative trend, and grey an insignificant trend. Coloured boxes show the regional domains: Pearl River Delta (PRD), Yangtze River Delta (YRD), North China Plain (NCP), Sichuan Basin (SCB), Hong Kong (HK), Taiwan (TW) and the Fenwei Plain (FWP).**
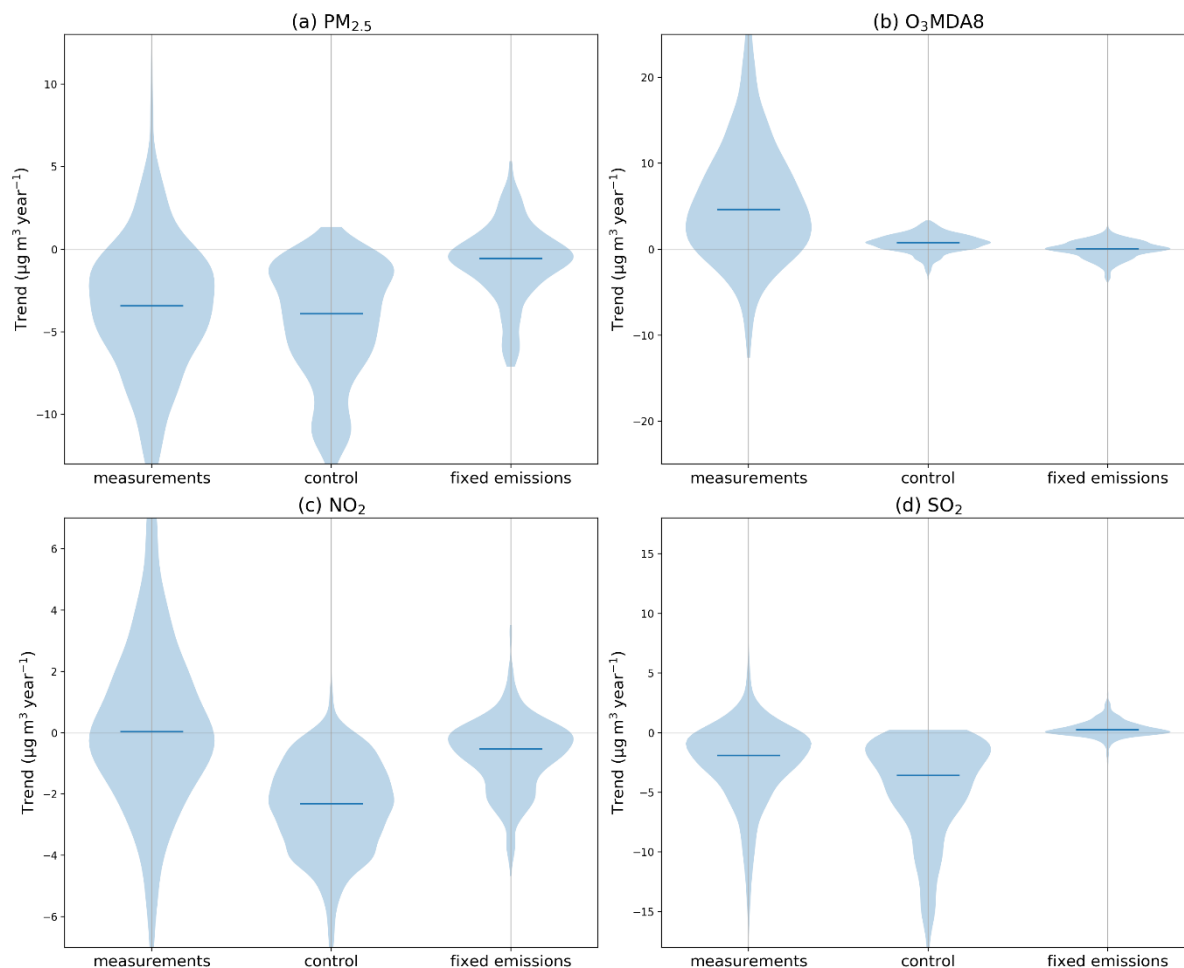
Figure 3. Comparison of measured and simulated concentration trends during 2015 to 2017. The left violin shows the measured trend, the centre shows the simulated trend with varying emissions and meteorology (control), and the right shows the simulated trends for the fixed emissions simulation. a) PM$_{2.5}$, b) O$_3$MDA8 , c) NO$_2$, d) SO$_2$. The solid line shows the median absolute trend, and the shaded area shows a smoothed relative frequency distribution.
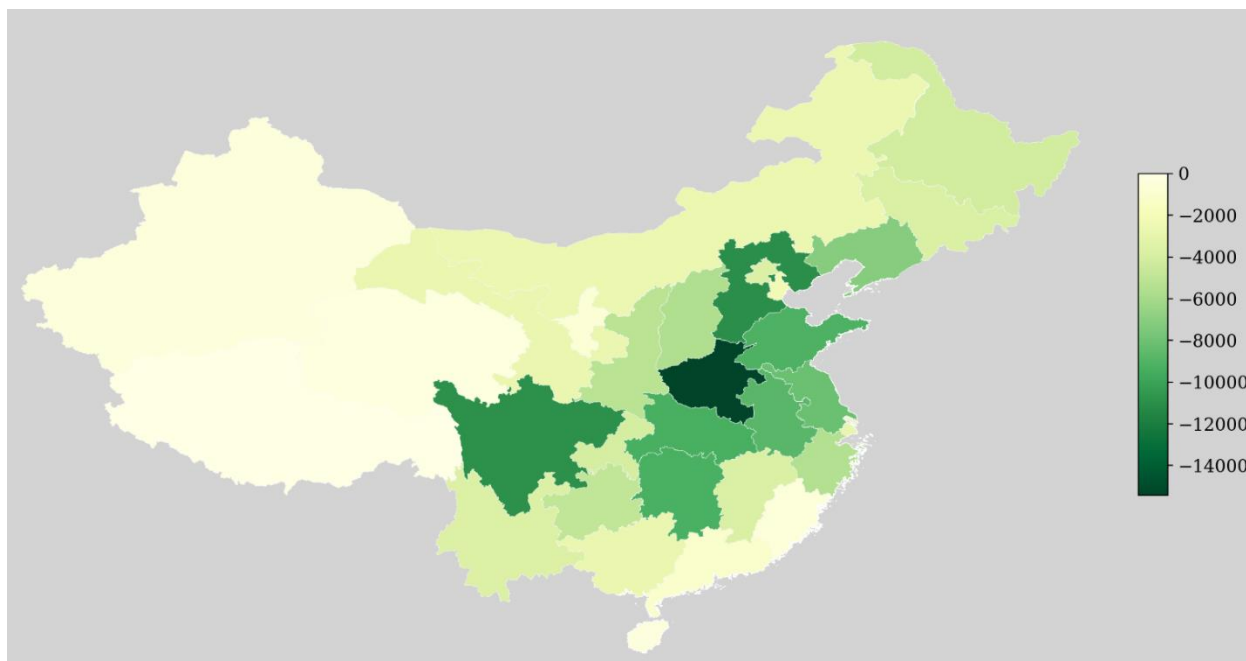
405

Figure 4. Simulated change during 2015-2017 in annual premature mortality per year due to changes in exposure to ambient PM$_{2.5}$. Results are shown at the province scale.